

Magnetization Distribution on Fractals and Percolation Lattices

R. Mélin

CRTBT-CNRS, 38042 Grenoble BP 166X cédex France

e-mail: melin@crtbt.polycnrs-gre.fr

Abstract

We study the magnetization distribution of the Ising model on two regular fractals (a hierarchical lattice, the regular simplex) and percolation clusters at the percolation threshold in a two dimensional imbedding space. In all these cases, the only fixed point is $T = 0$. In the case of the two regular fractals, we show that the magnetization distribution is non trivial below $T^* \simeq A^*/n$, with n the number of iterations, and A^* related to the order of ramification. The cross-over temperature T^* is to be compared with the glass cross-over temperature $T_g \simeq A_g/n$. An estimation of the ratio T^*/T_g yields an estimation of the order of ramification of bidimensional percolation clusters at the threshold ($C = 2.3 \pm 0.2$).

1 Introduction

We consider the problem of Ising spin systems on a family of fractals with a zero temperature fixed point. More especially, we consider the case of a hierarchical lattice, the regular simplex (regular fractals), and bidimensional percolation clusters at the percolation threshold. This problem has its origin in the pioner work of Mandelbrot [1]. The problem is also of an experimental interest because of the existence of random magnets with a fractal structure (see for instance [2]). As a byproduct, we derive a measure of the ramification order of percolating clusters. To do so, we compare to cross-over temperatures: 1) the glass cross-over temperature T_g 2) the magnetization distribution cross-over temperature T^* . The dominant behavior of the glass cross-over temperature was discovered in the 80's [3] [4]. This quantity is related to the correlation length of the magnet. Below T_g , the correlation length is larger than the system size, leading to a linear regime of the logarithm of the relaxation time as a function of the inverse temperature. Above T_g , the correlation length is smaller than the linear size of the cluster, leading to a parabolic behavior for the logarithm of the relaxation time as a function of the inverse temperature. This behavior is well established on a numerical basis [5]. The second cross-over temperature T^* was not much studied in the past. Below T^* [which is inverse proportional to the logarithm of the number of sites], the magnetization distribution is non Gaussian. These non Gaussian magnetization distributions also occur on the ferromagnetic Cayley tree [6], however with a different decay with the system size. More surprising is the appearance of similar magnetization distributions in magnetized spin glasses [7]. However, in real spin glasses, this non Gaussian magnetization distribution is not expected to vanish in the thermodynamic limit as it is the case on ferromagnetic systems. We first study the case of regular fractals (a hierarchical lattice and the regular simplex). We use the Swendsen algorithm to generate equilibrium states [8], and thus to calculate the magnetization distributions. In the case of the regular simplex, it is possible to determine the geometric origin of the different local maxima of the magnetization distribution at low temperatures. In section 4, we make a general argument to estimate the magnetization distribution cross-over scale, which is shown to be inverse proportional to the number of sites, and proportional to the ramification order C . In the case of percolating clusters, we calculate the magnetization distribution at low temperature. Averaging over the geometry, we can see the existence of finite size effects: the spin system is more ferromagnetic if one lowers the number of generations. We also studied the correlation between different equilibrium states, which gives us an other way to estimate T^* . Finally, we calculate the ration T_g/T^* , which yields an estimation of the ramification order of bidimensional percolation clusters. We end up with some concluding remarks.

2 A Hierarchical Lattice

The interest of hierarchical lattices is that the thermodynamics of the Ising model is exactly soluble on these structures. We consider the case of the hierarchical lattice built with the rules of figure 1. The coordination of every site is bounded above, which is not always the case for hierarchical lattices (for instance for the hierarchical diamond, in which case the coordination diverges in the thermodynamic limit). The number of sites of the hierarchical lattice of figure 1 is $N_n = 4 \cdot 6^n / 5 + 6/5$, whereas the end to end distance is $L_n = 4^{n-1}$, leading to the fractal dimension $\bar{d} = \ln 6 / \ln 4$.

An interesting aspect of hierarchical lattices is that their Yang and Lee zero can be calculated easily in the temperature plane. This was done in [10] in the case of the hierarchical diamond. The Yang and Lee zeros set is a Julia set. For comparison with the results of [10], we also calculate the Yang and Lee zeros of our hierarchical lattice. First, we need to derive recursion relations for the partition function.

2.1 Recursion for the Partition Function

The technique (standard for hierarchical lattices) consists in carrying out the trace over the spin variables at the smallest scales, and to derive the renormalization of the temperature and magnetic field. The partition function of the hierarchical lattice with one generation is

$$Z_1(\Sigma, \Sigma') = \sum_{\sigma_0, \sigma_1, \sigma_2, \sigma_3} e^{\beta J(\sigma_0 \Sigma + (\sigma_0 + \sigma_3)(\sigma_1 + \sigma_2)) + \sigma_3 \Sigma'} e^{\beta H(\sigma_0 + \dots + \sigma_3)}, \quad (1)$$

where the spins are pictured on figure 1. A straightforward calculation leads to

$$\begin{aligned} Z_1(\Sigma, \Sigma') &= 2 \left(e^{4\beta J} \cosh(\beta J(\Sigma + \Sigma') + 4\beta H) + e^{-4\beta J} \cosh \beta J(\Sigma + \Sigma') \right. \\ &\quad \left. + \cosh(\beta J(\Sigma - \Sigma') + 2\beta H) + \cosh(\beta J(\Sigma - \Sigma') - 2\beta H) \right. \\ &\quad \left. + 2 \cosh \beta J(\Sigma - \Sigma') + 2 \cosh(\beta J(\Sigma + \Sigma') + 2\beta H) \right). \end{aligned} \quad (2)$$

The partition function $Z_1(\Sigma, \Sigma')$ can be rewritten under the form

$$Z_1(\Sigma, \Sigma') = \mathcal{N} e^{\beta \tilde{J} \Sigma \Sigma'} e^{\beta \tilde{H}(\Sigma + \Sigma')}. \quad (3)$$

We have introduced here three parameters \mathcal{N} , \tilde{J} and \tilde{H} for three distinct partition functions $Z(+, +)$, $Z(-, -)$ and $Z(+, -) = Z(-, +)$. The partition function can thus be consistently be brought under the form (3). The identification of (2) and (3) leads to

$$\mathcal{N} = \left(Z_1(+, +) Z_1(+, -)^2 Z_1(-, -) \right)^{1/4} \quad (4)$$

$$\exp \beta \tilde{J} = \frac{\mathcal{N}}{Z_1(+, -)} = \frac{(Z_1(+, +) Z_1(-, -))^{1/2}}{\mathcal{N}} \quad (5)$$

$$\exp 4\beta \tilde{H} = \frac{Z_1(+, +)}{Z_1(-, -)}. \quad (6)$$

In the case of a zero magnetic field, we obtain

$$Z_n(J) = \mathcal{N}^{6^{n-1}} Z_{n-1}(\tilde{J}), \quad (7)$$

with

$$\mathcal{N}^2 = 8 (\cosh 6\beta J + 3 \cosh 2\beta J + 4) (\cosh 4\beta J + 2 \cosh 2\beta J + 1), \quad (8)$$

and

$$e^{2\beta\tilde{J}} = \frac{\cosh 6\beta J + 3 \cosh 2\beta J + 4}{2 (\cosh 4\beta J + 2 \cosh 2\beta J + 1)}. \quad (9)$$

The renormalization equation (9) has only one fixed point: $J = 0$, so that the spin system is always disordered at any finite temperature in the thermodynamic limit.

2.2 Digression: Yang and Lee zeros in the Temperature Plane

We now calculate the Yang and Lee zeros in the temperature plane. This is not the main subject of this paper, but it is interesting to compare with existing results on the hierarchical diamond, where the Yang and Lee zero in the temperature plane form a Julia set [10]. We work in the plane of the variable $z = \exp 2\beta J$ and invert the relation (9), which leads to a polynomial of degree 6:

$$z^6 - 2\tilde{z}z^5 + (3 - 4\tilde{z})z^4 + 4(2 - \tilde{z})z^3 + (3 - 4\tilde{z})z^2 - 2\tilde{z}z + 1 = 0, \quad (10)$$

If z is a solution of (10), $1/z$ is a solution too, so that the set of zeros of the partition function is invariant under the inversion $z \rightarrow 1/z$. In order to compute the set of zeros of the partition function, we use the methods of [10], that is we start from a given point in the complex plane, we calculate the zeros of (9), choose one solution among the six zeros at random, and reiterate. The zeros are computed using a Laguerre's method [11]. The resulting set is independent on the initial value of z , as far as one eliminates the first zeros. The result is plotted on figure 2. The set of zeros are concentrated on lines, which intersect the real axis in the vicinity of the point $z = 0$. A zoom in the vicinity of $z = 0$ reveals that the density of zeros vanishes as one approaches the origin (see figure 3). Contrary to the case of the hierarchical diamond, the Lee and Yang zeros are concentrated on lines in the $z = \exp 2\beta J$ plane, whereas the Julia set of the hierarchical diamond is a fractal.

2.3 Glass Cross-over Temperature

The glass temperature cross-over T_g is related to the decay of the correlation function from one end of the fractal to the other [3] [5] [9]. Since the Ising model is soluble on the hierarchical lattice, it is easy to get the behavior of the correlation length between the extremal sites as

a function of the number n of iterations and the temperature. We call x the dimensionless inverse temperature $x = \beta J$. In the low temperature regime, we get from equation (9) $x_{n+1} \simeq x_n - \ln 2/2$, where x_n is the value of x after n renormalization steps. In the low temperature regime, $x_{n+1} \simeq 2x_n^4$. The limit between the high and low temperature regimes corresponds to the minimum κ of $2x^4 - x + \ln 2/2$. We find $\kappa \simeq 0.59$. The correlation between the two extremal sites is nothing but

$$\langle \Sigma \Sigma' \rangle = \frac{1}{Z[0]} \frac{\partial}{\partial \mu} Z[\mu = 0], \quad (11)$$

where

$$Z[\mu] \propto \sum_{\Sigma, \Sigma'} e^{\beta J_n \Sigma \Sigma'} e^{\mu \Sigma \Sigma'}, \quad (12)$$

so that the correlation is simply $\langle \Sigma \Sigma' \rangle = \tanh \beta J_n$, which decreases from unity to zero as n increases from 1 to $+\infty$. The cross-over temperature T_g corresponds to $x_n > \kappa$ and $x_{n+1} < \kappa$, leading to the dominant behavior of the glass cross-over temperature

$$T_g = \frac{2J}{n \ln 2}. \quad (13)$$

2.4 Magnetization Distribution

The magnetization distribution becomes non gaussian below a temperature T^* . This is due to the existence of macroscopic domains that are weakly connected to the rest of the structure. The temperature cross-over T^* is evaluated in section 4 in a more general context, so that we do not reproduce the argument here in the case of the hierarchical lattice. The result in the case of the hierarchical lattice is

$$T^* = \frac{4J}{n \ln 6}, \quad (14)$$

where we have kept only the dominant behavior for large n . The results for the magnetization distribution are plotted on figure 4 for $n = 4$. Using (14) for $n = 4$, we get $T^* \simeq 0.55$, which is consistent with the data of figure 4. Notice that, in this case, $T_g < T^*$.

3 Regular Simplex

The regular simplex recursion is plotted on figure 5. The number of sites is $N_n = 3^n$, and the corresponding distance is $L_n = 2^n$, so that the fractal dimension is $\bar{d} = \ln 3 / \ln 2$.

3.1 Recursion for the Partition Function

The partition function in a zero external field can be calculated recursively by calculating the trace over the spins at the deepest generation. With the notations of figure 5, the partition function is

$$Z(\Sigma_1, \Sigma_2, \Sigma_3) = \exp(\beta J(\Sigma_1(\sigma_{12} + \sigma_{13}) + \Sigma_2(\sigma_{21} + \sigma_{23}) + \Sigma_3(\sigma_{31} + \sigma_{32})) \quad (15)$$

$$\exp(\beta J(\sigma_{31}\sigma_{32} + \sigma_{21}\sigma_{23} + \sigma_{12}\sigma_{13})). \quad (16)$$

We look for Z under the form

$$Z(\Sigma_1, \Sigma_2, \Sigma_3) = \mathcal{N} \exp(\beta \tilde{J}(\Sigma_1 \Sigma_2 + \Sigma_2 \Sigma_3 + \Sigma_1 \Sigma_3)). \quad (17)$$

The renormalized form of Z has two parameters (\mathcal{N} and \tilde{J}), for two distinct equations: one for $(\Sigma_1, \Sigma_2, \Sigma_3) \in \mathcal{S}_1$, and the other for $(\Sigma_1, \Sigma_2, \Sigma_3) \in \mathcal{S}_2$, with

$$\mathcal{S}_1 = \{(+, +, +), (-, -, -)\} \quad (18)$$

$$\mathcal{S}_2 = \{(+, +, -), (+, -, +), (-, +, +), (-, -, +), (-, +, -), (+, -, -)\}. \quad (19)$$

The parameters \mathcal{N} and \tilde{J} are simply given by

$$\mathcal{N} = (Z(+, +, +)Z(+, +, -))^{1/4} \quad (20)$$

$$\beta \tilde{J} = \frac{1}{4} \ln \left(\frac{Z(+, +, +)}{Z(+, +, -)} \right). \quad (21)$$

Carrying out the trace over the σ variables leads to

$$Z(+, +, +) = 27e^{-3\beta J} + 27e^{\beta J} + 9e^{5\beta J} + e^{9\beta J} \quad (22)$$

$$Z(+, +, -) = 3e^{-7\beta J} + 19e^{-3\beta J} + 33e^{\beta J} + 9e^{5\beta J}. \quad (23)$$

In the high temperature regime, the coupling constant renormalization is $\tilde{x} \simeq x^3$ and, in the low temperature regime, $\tilde{x} \simeq x - (\ln 3)/2$, where $x = \beta J$. The cross-over between the high and low temperature regime is $x = \kappa$, with κ the minimum of $x^3 - x + (\ln 3)/2$ ($\kappa \simeq 0.58$).

The correlation function is

$$\langle \Sigma_1 \Sigma_2 \rangle = \frac{1}{Z[0]} \frac{\partial}{\partial \mu} Z[\mu = 0], \quad (24)$$

with

$$Z[\mu] \propto \sum_{\Sigma_1, \Sigma_2, \Sigma_3} \exp(x_n(\Sigma_1 \Sigma_2 + \Sigma_1 \Sigma_3 + \Sigma_2 \Sigma_3)) \exp(\mu \Sigma_1 \Sigma_2) = \frac{e^{3x_n} - e^{-x_n}}{e^{3x_n} + 3e^{-x_n}}, \quad (25)$$

from what we deduce the dominant behavior of the cross-over temperature scale

$$T_g = \frac{2J}{n \ln 3}. \quad (26)$$

3.2 Magnetization Distribution

The magnetization distribution is plotted on figure 6 for various temperatures. Again, we do not reproduce the calculation of the magnetization cross-over temperature T^* since a general argument is developed in section 4. The result for the dominant behavior of T^* in the limit of large n is

$$T^* = \frac{6J}{n \ln 3}. \quad (27)$$

In the case $n = 7$ (which corresponds to figure 6), we have $T^* \simeq 0.8$, which is consistent with the data of figure 6. Notice also that, in the low temperature regime, when the non gaussian structure of the magnetization distribution is fully developed, it is possible to identify the origin of the different local maxima of $P(m)$. To do so, we carry out a low temperature expansion of the magnetization distribution around the broken symmetry state $m = 1$, up to the order μ^3 , where $\mu = e^{-\beta J}/(e^{\beta J} + e^{-\beta J}) \simeq e^{-2\beta J}$. The result is

$$P(m) = (1 - n\mu^2 - A\mu^3)\delta(1 - m) + 3\mu^2 \sum_{p=0}^{n-1} \delta(m - 1 + 2 \cdot 3^{p-n}) \quad (28)$$

$$+ \mu^3 \left[\sum_{p=0}^{n-2} (3^{n-p} - 3)\delta(m - 1 + 2 \cdot 3^{p-n}) + 6 \sum_{M \in \mathcal{A}} \delta\left(1 - \frac{2M}{3^n}\right) \right] + o(\mu^3). \quad (29)$$

A is a normalization constant and the set \mathcal{A} is

$$\mathcal{A} = \{M \in \langle 1, \dots, [N/2] \rangle, \exists k, \exists l, 0 \leq l < k, M = 3^k \pm 3^l\}. \quad (30)$$

We can recognize on figure 6 the contributions from $m = 1/3, 1/9, 1/27$ but also from $m = 1/3 \pm 1/27, 1/3 \pm 1/9, 1/9 \pm 1/27$.

4 General Argument for Regular Fractals with a Zero Temperature Transition

We first recall what happens on the Cayley tree [6], where there exists also a glassy cross-over, with $T_g \propto J/\ln n$, where n is the number of generations of the tree, and also a crossover in the magnetization distribution, with $T^* \propto J/\ln n$. It is possible to derive exact recursion relations for the average magnetization, to solve the recurrence, and to obtain the temperature cross-over T^* . The cross-over temperature is interpreted as follows: below T^* , there exists less than one broken bound on a path connecting the center of the tree to the leaves, which leads to the criterium for the magnetization distribution cross-over temperature:

$$n\mu \simeq 1. \quad (31)$$

Taking the logarithm leads to $T^* \propto J/\ln n$.

In the case of fractals, there are not bifurcations, so that the criterium corresponding to (31) is

$$\mu^C N_n \simeq 1, \quad (32)$$

which means that, at the cross-over, there exists only C broken bounds on the graph, where C is the number of bounds that need to be cut to isolate a p generations fractals in the bulk of a n generations fractal. This is the ramification order. We thus obtain

$$T^* = \frac{2JC}{\ln N_n}. \quad (33)$$

In order to check this equation, we come back to the case of the hierarchical lattice, where we obtained recursively the partition function in an external magnetic field. We impose a small magnetic field, and calculate the partition function in the presence of the small magnetic field, and deduce the average magnetization numerically as a function of the number of generations. For a given number of generation, we look for the temperature for which the magnetization is a given constant. We thus obtain the curve $\beta^*(n)$, which is expected to be a straight line from equation (33). This is indeed the case, as shown on figure 7, which validates the previous heuristic argument.

5 Percolation Clusters at the Threshold

5.1 Glass cross-over temperature

Percolation clusters at the percolation threshold were studied in the past as an exemple of critical dynamics, with a glassy-like dynamics below T_g [3] [5] [9]. The glass cross-over temperature T_g is evaluated in [3] with the argument that below T_g , the correlation length [12]

$$\xi_T = \exp\left(\frac{2J\nu_p}{T}\right) \quad (34)$$

is inferior to the linear size of the cluster. One gets easily [3]

$$T_g = \frac{2J\bar{d}\nu_p}{\ln N}, \quad (35)$$

where N is the number of sites of the percolation cluster.

5.2 Magnetization Distribution

The magnetization distribution of a single cluster at low temperatures looks like the one of regular fractals, apart from the fact that the localization of the local minima depends on

the geometry and is not easy to localize. For instance, we generated a percolation cluster at threshold in a bidimensional imbedding space ($p_c = 0.593$). The corresponding low temperature magnetization distribution is plotted on figure 8 for various temperatures. We show on figure 9 two configurations belonging to the local maximum with a normalized number of up spins $N_\uparrow/N \simeq 0.38$. The interpretation of the magnetization distribution thus depends crucially on the geometry. It is therefore legitimate to ask whether the local maxima structure persists after averaging over the geometry. The answer is ‘no’: we plotted on figure 10 the magnetization distribution averaged over the geometry for different temperature. We observe no local maxima. If the temperature increases, the weight of the ferromagnetic maximum decreases, whereas the tail of the distribution increases, which is consistent with the fact that the magnetization distribution is gaussian in the high temperature regime.

Moreover, by averaging over the geometry, we can adress the question of finite size effects. We plotted on figure 11 the distribution of magnetization for two different sizes at the same temperature. We see that the small clusters have a more pronounced ferromagnetic peak, which is in agreement with the fact that T^* decreases with the system size.

5.3 Correlations

We wish to analyze the correlation between the different spin configuration at a given temperature. To do so, we introduce n replica of the spin system. We call $q_i^{(\alpha)} \in \{0, 1\}$ the value of the Potts variables in the replica α ($1 \leq \alpha \leq n$), and we consider the following correlation:

$$R_N(q, T) = \frac{1}{q} \sum_{i=1}^N \frac{2}{n(n-1)} \sum_{\langle \alpha, \beta \rangle} q_i^{(\alpha)} q_i^{(\beta)} \quad (36)$$

for a given geometry with a given magnetization (all the replica have the same magnetization). The variable q is the average magnetization:

$$\forall \alpha, q = \frac{1}{N} \sum_{i=1}^N q_i^{(\alpha)}. \quad (37)$$

The correlation $R_N(q, T)$ in a sector of given magnetization is nothing but a kind of Edwards-Anderson order parameter in a subspace of given magnetization. In the high temperature regime, q_i^α is 0 with a probability 1/2 and 1 with a probability 1/2, so that the average of $q_i^{(\alpha)} q_j^{(\alpha)}$ is 1/4, so that

$$R_N(q, t) = \frac{N}{4q} \quad (38)$$

if $T > T^*$. We are interested in the variations of R for a given magnetization as a function of the temperature. These variations are plotted on figure 12 for a given geometry. The

magnetization is $q = N_{\uparrow}/N \simeq 0.38$. The four different curves are plotted for neighboring magnetizations. As expected, R tends to 0.38 above T^* . The estimation of T^* from this technique is coherent with the estimation from the analysis of the magnetization distribution (see figure 8).

5.4 Evaluation of the Ramification Order of Percolating Clusters

We know from two different methods that the cross-over temperature T^* for $N = 2660$ sites is about $T^* \simeq 0.6$. From this data, we can deduce the ramification order C , which, in the case of regular fractals was interpreted as the number of links to be cut to isolate a p generations fractal inside a n generations fractal ($n > p$). We deduce from (33) and (35) that

$$\frac{T^*}{T_g} = \frac{C}{\nu_p \bar{d}}. \quad (39)$$

On the other hand, we know that $\nu_p \simeq 1.3$ in a bidimensional imbedding space [13], and that $\bar{d} = 1.78 \pm 0.02$ [14]. With $N = 2660$ sites, we evaluate $T_g \simeq 0.6$ from (35). Using (39), we get $C = 2.3 \pm 0.2$. The uncertainty comes from the uncertainty in the location of the cross-over temperature T^* . This result is in agreement with the fact that the order of ramification of percolating clusters is believed to be finite and superior to two (percolating clusters are not quasi one dimensional) [15].

6 Conclusion

We have studied the magnetization distribution on fractals with a zero temperature transition. Below a temperature inverse proportional to the logarithm of the number of sites, and proportional to the order of ramification, the magnetization is not trivial, with local maxima. This is due to the fact that it is possible to cut the graph into many large parts, by breaking only a small number of links. We have introduced a magnetization-dependent Edwards-Anderson order parameter, the variations of which are correlated with the magnetization distribution. It would be interesting to have an analytical proof of this fact. We have shown in that the cross-over temperature T^* of percolating clusters is related to the order of ramification of the structure. We find $C = 2.3 \pm 0.2$ for bidimensional percolation clusters. The cross-over temperature T^* can be estimated in two different ways: 1) by calculating directly the probability distribution at different temperatures 2) by calculating the correlation between equilibrium states with a given magnetization. Our result is in agreement with the fact that the percolation cluster at threshold is not quasi one dimensional (which was known a long time ago!). However, it is clear that our method to determine the order of ramification is not accurate,

since one has to estimate a cross-over temperature, which is determined up to a certain uncertainty. It would be interesting to generalize this study to magnetized spin glass phases. This will be done in a near future.

I acknowledge J.C. Anglès d'Auriac who lent me his Swendsen program, and I thank B. Douçot for comments on the manuscript.

References

- [1] Mandelbrot: *Fractal, Chance and Dimension* (Freeman, San Francisco, 1977).
- [2] T. Nakayama, K. Yukabo and R.L. Orbach, *Rev. Mod. Phys.* 66, 381 (1994).
- [3] R. Rammal and A. Benoit, *J. Physique Lett.* 46, L 667 (1985).
- [4] C.L. Henley, *Phys. Rev. Lett.* 18, 2030 (1981).
- [5] R. Rammal and A. Benoit, *Phys. Rev. Lett.* 55, 649 (1985).
- [6] R. Mélin, J.C. Anglès d'Auriac, P. Chandra and B. Douçot, submitted to *J. Phys. A.*, cond-mat/9509035.
- [7] J.M. Carlson, J.T. Chayes, L. Chayes, J.P. Sethna and D.J. Thouless, *J. Stat. Phys.* 61, 987 (1990).
- [8] R.H. Swendsen and J.S. Wang, *Phys. Rev. Lett.* 57, 2606 (1986); *Phys. Rev. Lett.* 58, 86 (1987). See also R.H. Swendsen, J.S. Wang and A.M. Ferrenberg in *The Monte Carlo Method in Condensed Matter Physics*, K. Binder (Ed.), Topics in Applied Physics 71, Springer-Verlag, Berlin-Heidelberg- New York (1992).
- [9] R. Rammal, *J. Physique* 46, 1837 (1985).
- [10] B. Derrida, L. De Seze and C. Itsykson, *J. Stat. Phys.* 33, 559 (1983).
- [11] W.H. Press, S. A. Teukolsky, W. T. Vetterling and B. P. Flannery, *Numerical recipes in C*, Cambridge University Press (1992).
- [12] A. Coniglio, *Phys. Rev. Lett.* 46, 250 (1981).
- [13] D. Stauffer, *Phys. Rep.* 54, 2 (1979).
- [14] H.E. Stanley, R.J. Birgeneau, P.J. Reynolds and F. Nicoll, *J. Phys. C* 9, L553 (1976).
- [15] S. Kirkpatrick in *Les Houches Summer School on Ill Condensed Matter Physics*, edited by R. Balian, R. Maynard and G. Toulouse (North Holland, Amsterdam, 1979).

Figure captions

Figure 1:

Construction of the hierarchical lattice. At the $n = 0$ step, we start with two sites connected. After one step, the lattice contains 6 sites. At each step, the links are transformed as in the $n = 0 \rightarrow n = 1$ transformation.

Figure 2:

Set of zeros of the partition function in the plane $z = \exp 2\beta J$. We have plotted 39000 zeros calculated by the procedure described in the text. 1000 zeros have been eliminated.

Figure 3:

Zoom of the set of zeros in the vicinity of the origin, for 19000 zeros of the partition function. The density of points corresponds to the density of zeros. The density of zeros vanishes in the vicinity of the origin.

Figure 4:

Magnetization distribution for the hierarchical lattice with 4 generations. For clarity, the plots have been shifted along the y axis. 750000 iterations of Swendsen algorithm were carried out.

Figure 5:

Construction of the regular simplex.

Figure 6:

Magnetization distribution for the regular simplex with 7 generations. For clarity, the plots have been shifted along the y axis. 750000 iterations of Swendsen algorithm were carried out.

Figure 7:

Inverse temperature cross-over as a function of the number of generations for the hierarchical lattice. The cross-over is such that the average magnetization is some constant, the two extremal spins being frozen in the up direction. The constant is taken equal to 0.02.

Figure 8:

Magnetization distribution for a percolation cluster of size $N = 2660$ sites (this cluster is pictured on figure 9). The temperature is $T = 0.34, 0.42, 0.50, 0.58, 0.66, 0.74$. 750000 iteration of the Lanczos algorithm were carried out.

Figure 9:

Two spin configurations in the peak $N_{\uparrow}/N \simeq 0.38$.

Figure 10:

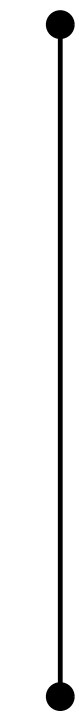
Magnetization distribution averaged over the geometry. The clusters are generated in a 60x60 box, and 100000 steps of Swendsen algorithm are carried out. For $T = 0.4(0.3, 0.5)$, 106(200, 58) different geometries were generated. Notice the semi-log scale.

Figure 11:

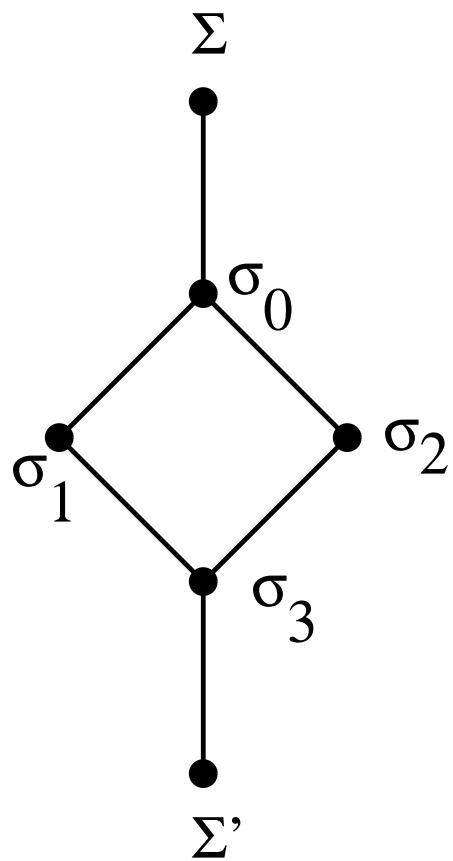
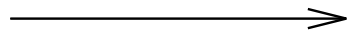
Magnetization distribution averaged over the geometry. The clusters are generated in a 60x60 box and a 25x25 box, and 100000 steps of Swendsen algorithm are carried out. The temperature is $T = 0.25$.

Figure 12:

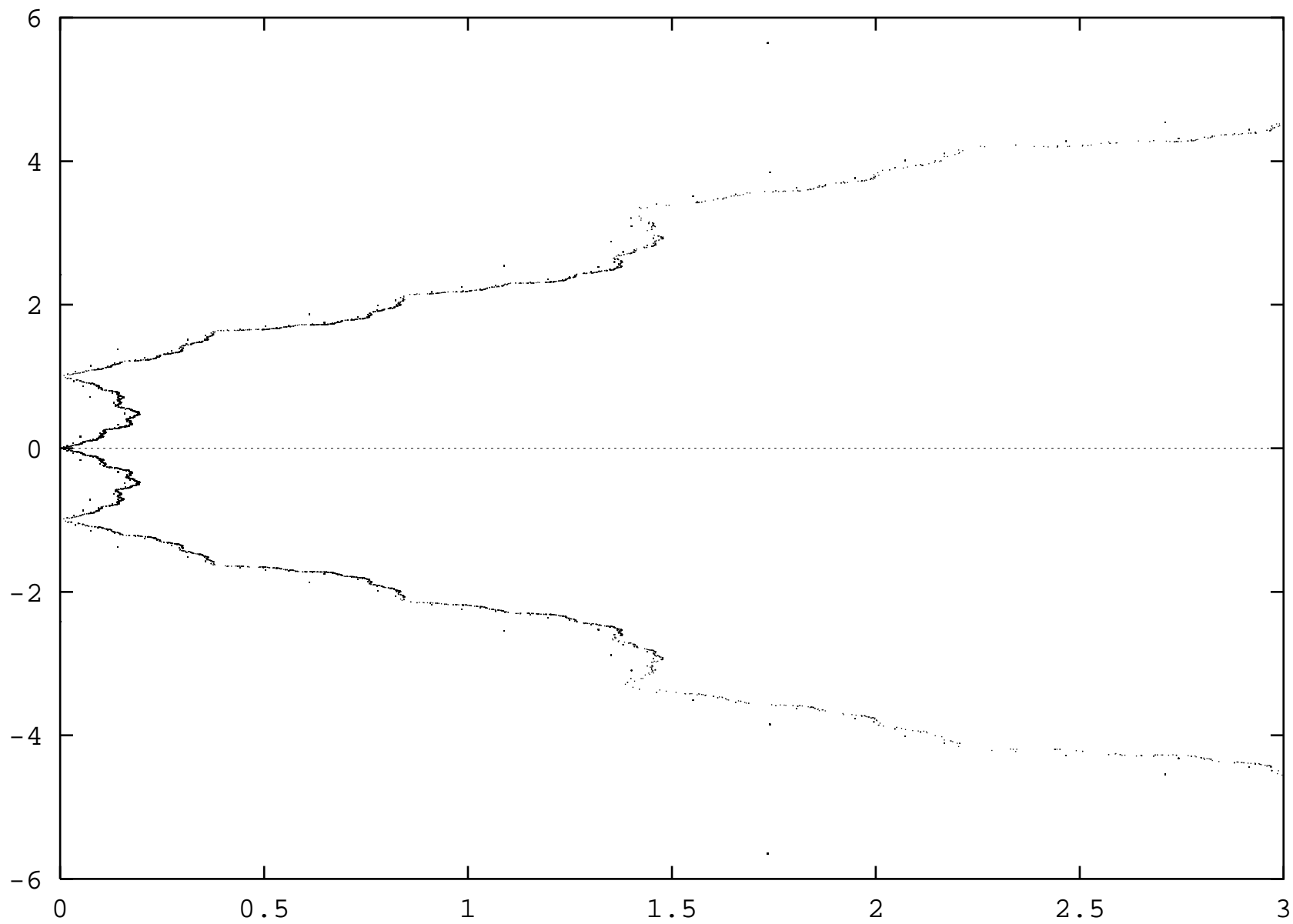
Variations of the correlation R as a function of the temperature for the cluster of figure 9. The average number of up spins is chosen to be around 0.38.

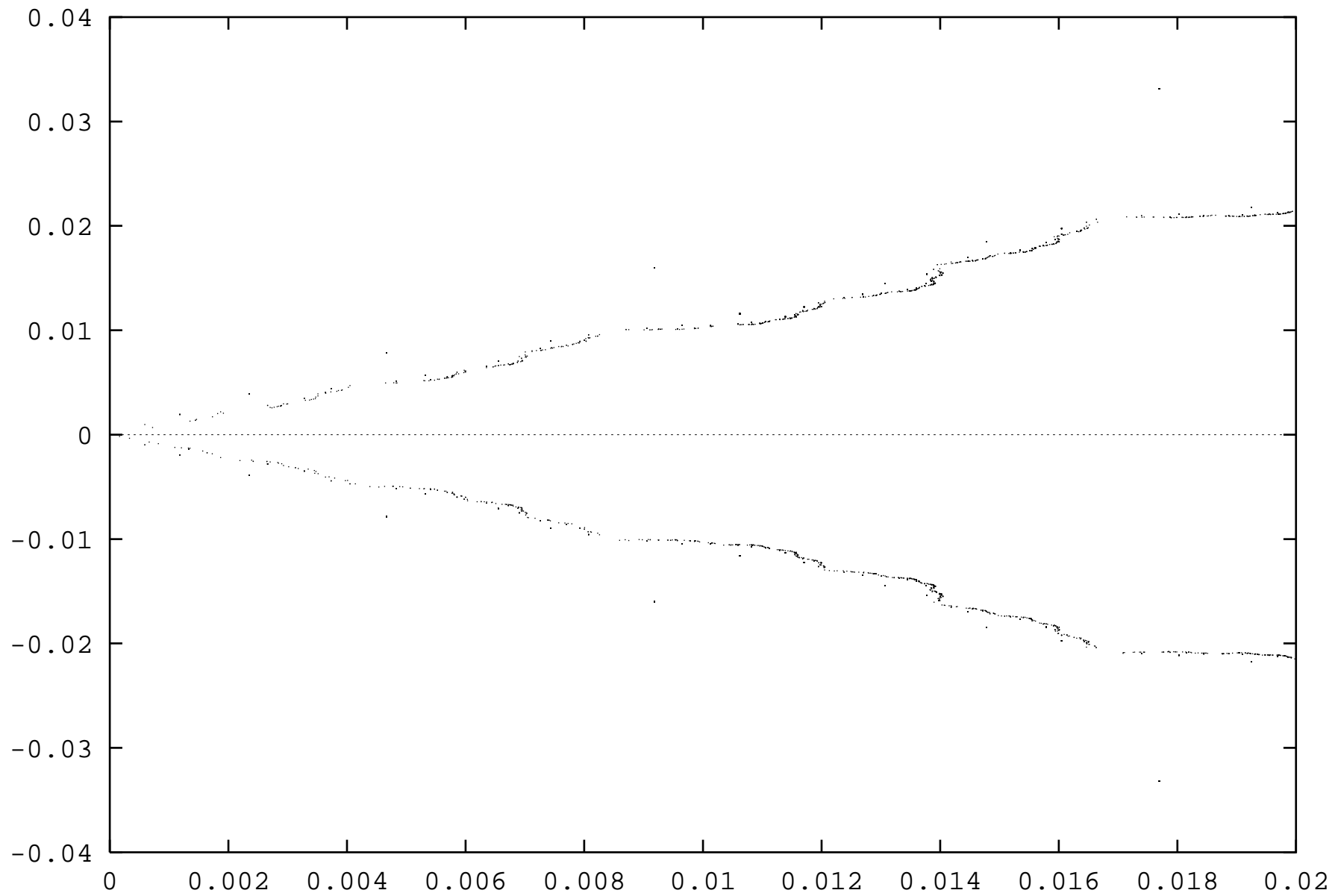


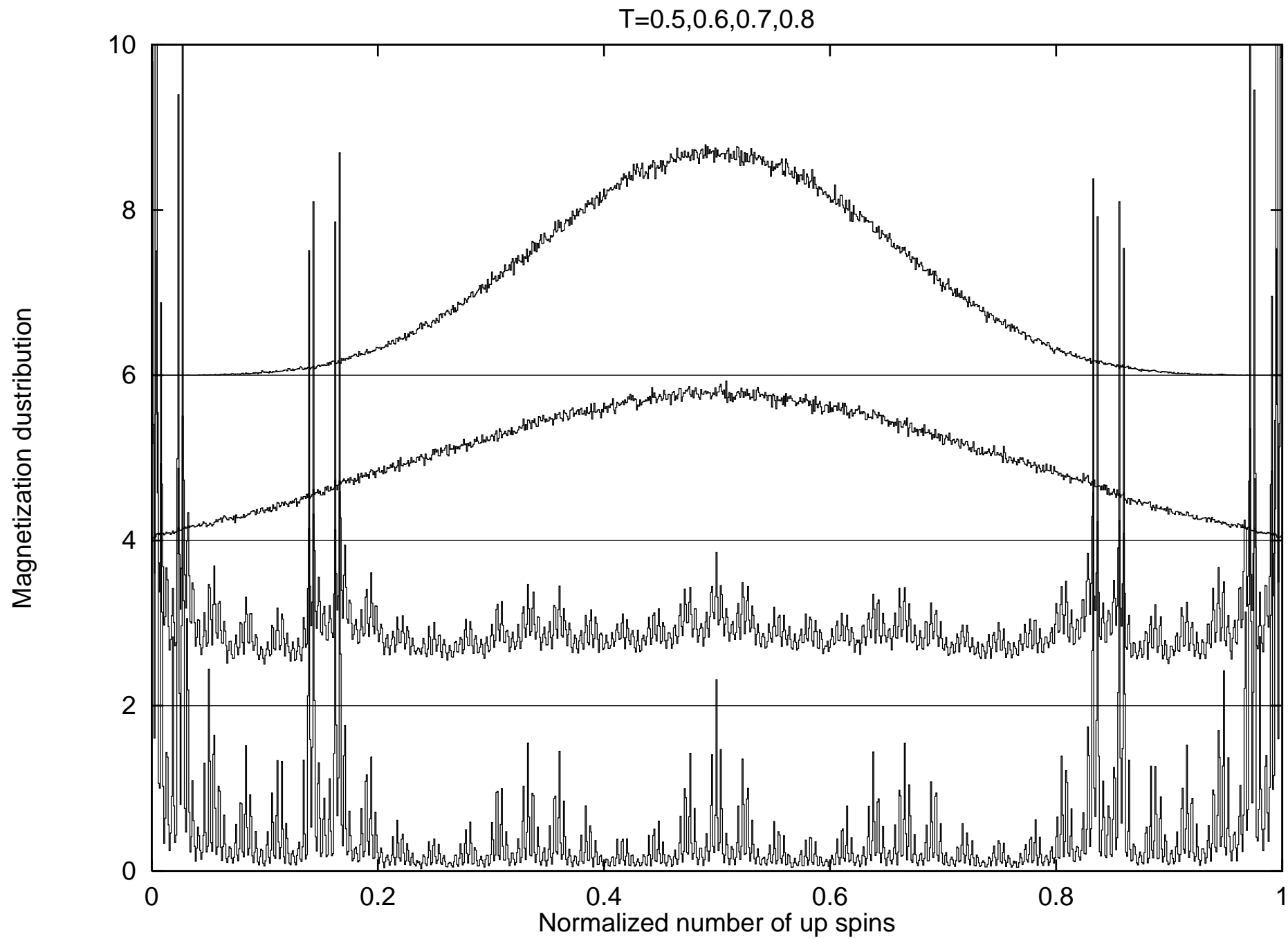
$n=0$

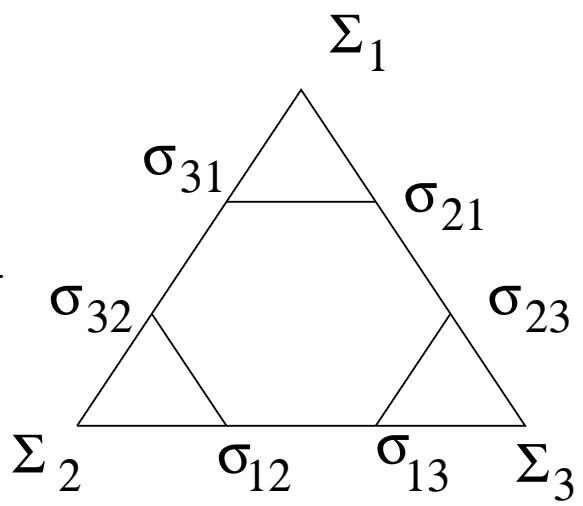
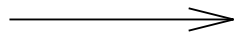
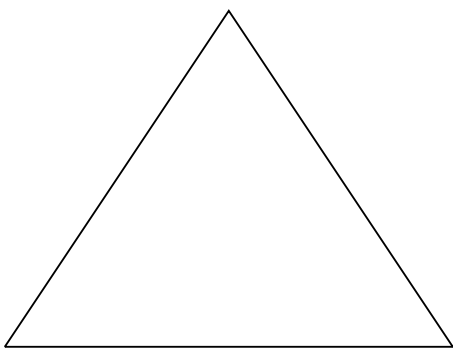


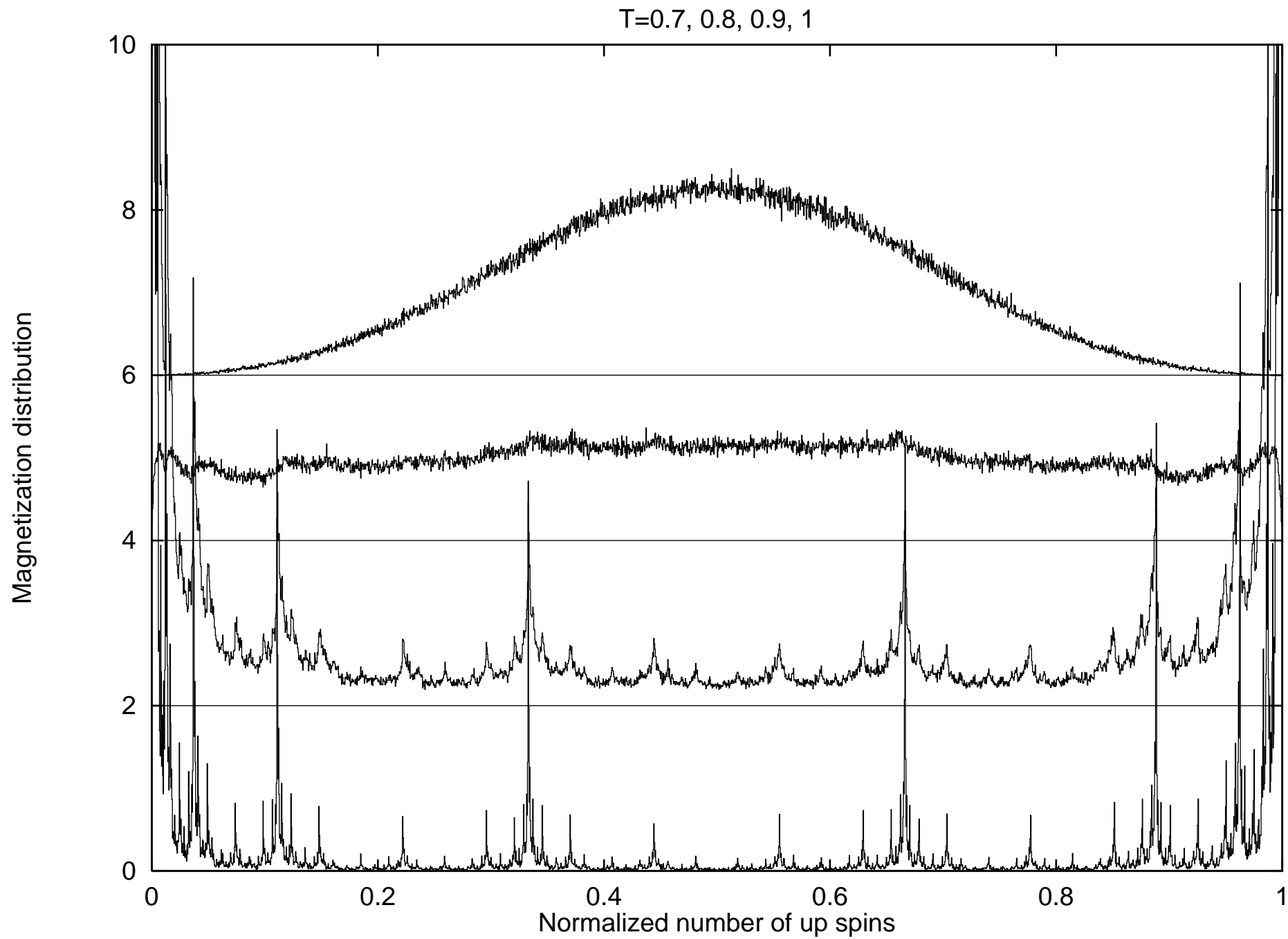
$n=1$

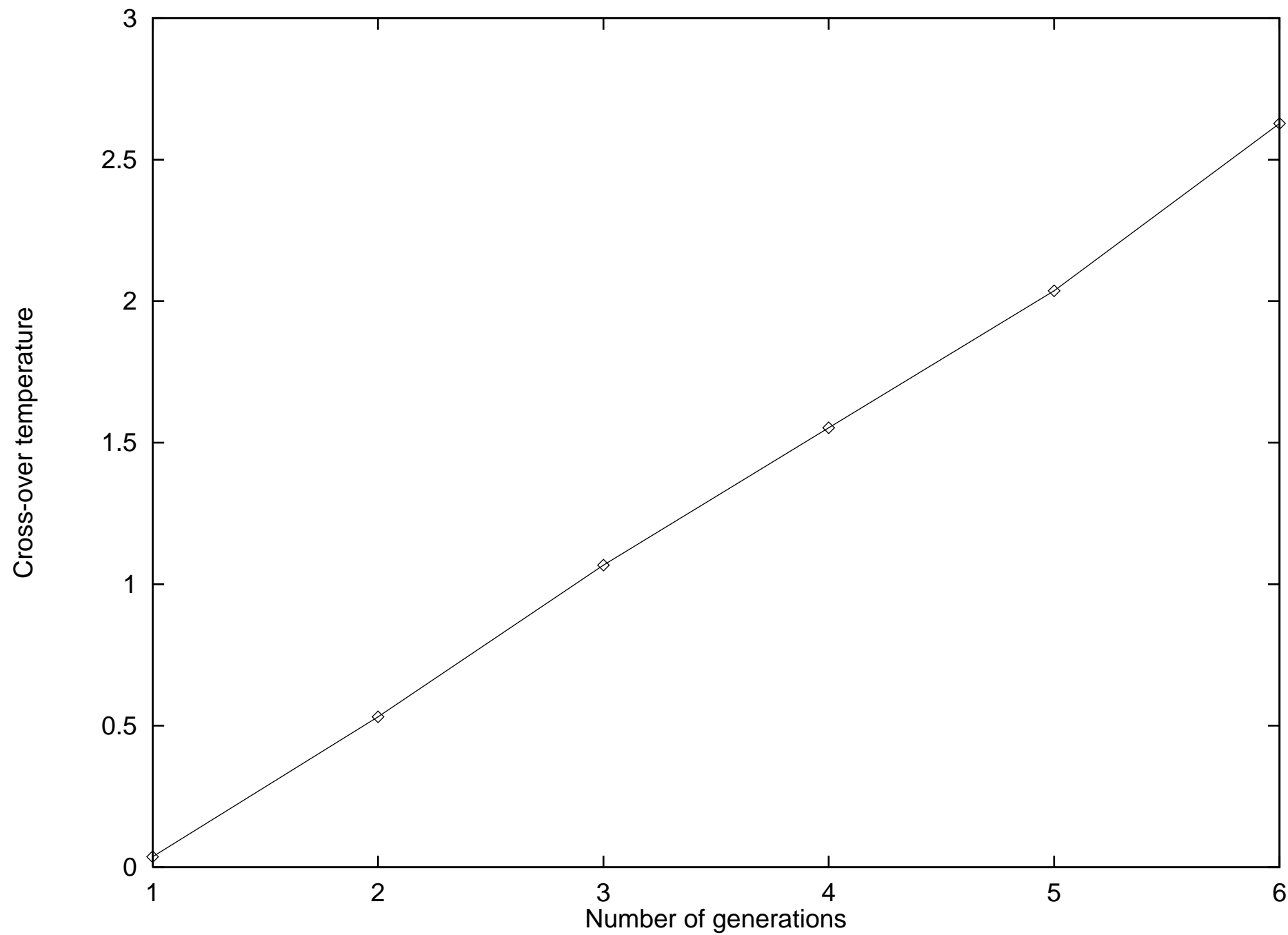




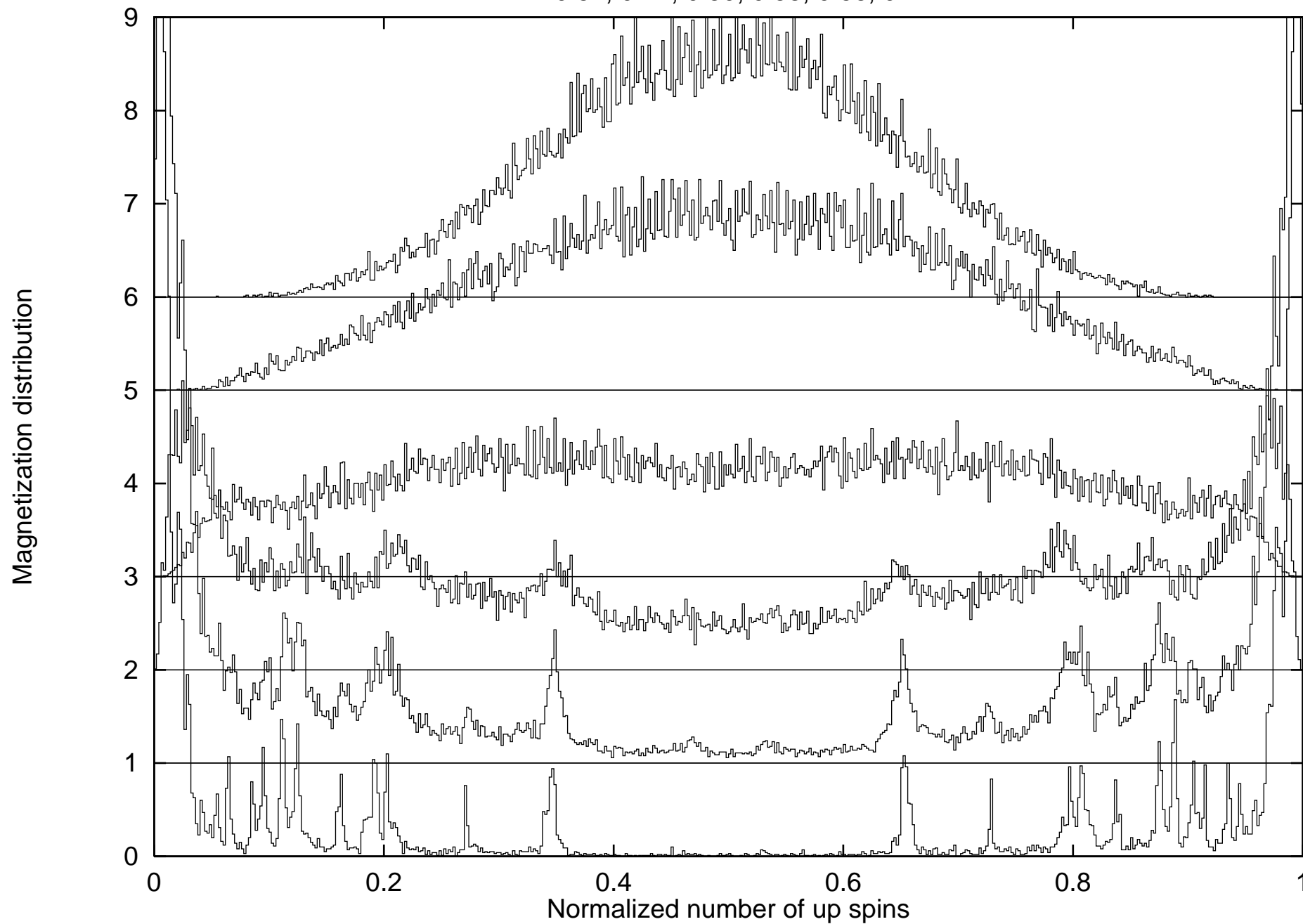


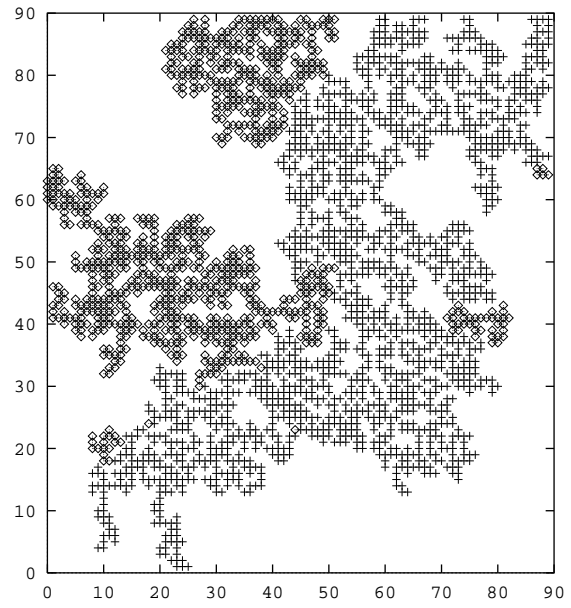
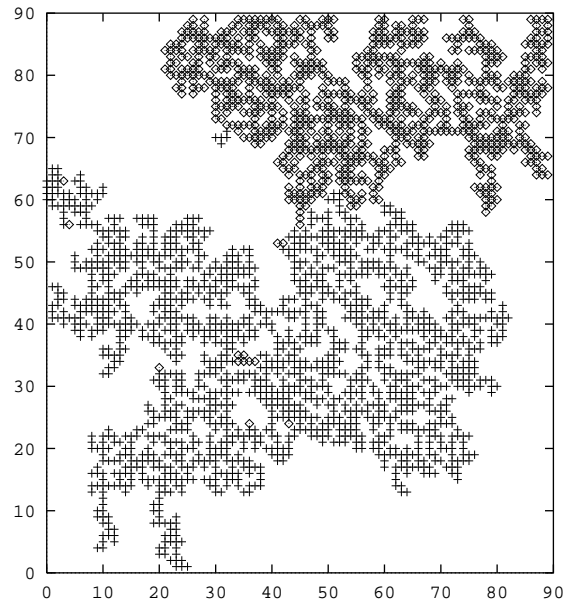


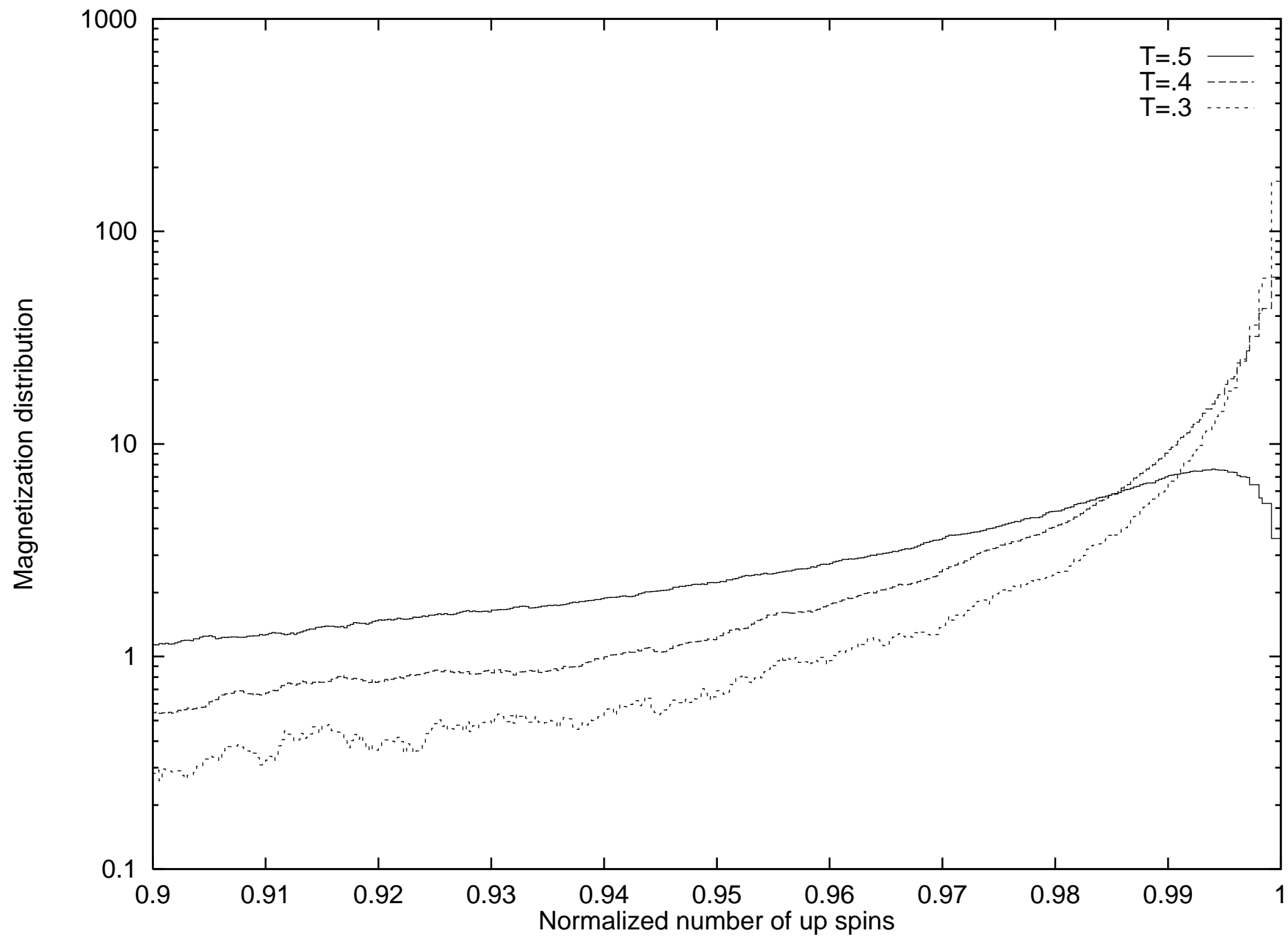




$T=0.34, 0.42, 0.50, 0.58, 0.66, 0.74$







T=0.5

